

The Form and Evolution of the Clustering of QSO Heavy-Element Absorption-Line Systems

Jean M. Quashnock

University of Chicago, Department of Astronomy and Astrophysics, 5640 South Ellis, Chicago, IL 60637

and

Daniel E. Vanden Berk¹

University of Texas, McDonald Observatory, RLM 15.308, Austin, TX 78712-1083;
jmq@oddjob.uchicago.edu, danvb@astro.as.utexas.edu

ABSTRACT

We have analyzed the clustering of C IV and Mg II absorption-line systems on comoving scales r from 1 to 16 h^{-1} Mpc, using an extensive catalog of heavy-element QSO absorbers with mean redshift $\langle z \rangle_{\text{C IV}} = 2.2$ and $\langle z \rangle_{\text{Mg II}} = 0.9$. We find that, for the C IV sample as a whole, the absorber line-of-sight correlation function is well-fit by a power law of the form $\xi_{\text{aa}}(r) = (r_0/r)^\gamma$, with maximum-likelihood values of $\gamma = 1.75^{+0.50}_{-0.70}$ and comoving $r_0 = 3.4^{+0.7}_{-1.0} h^{-1}$ Mpc ($q_0 = 0.5$). The clustering of absorbers at high redshift is thus of a *form* that is consistent with that found for galaxies and clusters at low redshift, and of amplitude such that absorbers are correlated on scales of galaxy clusters. We also trace the *evolution* of the mean amplitude $\xi_0(z)$ of the correlation function, as a function of redshift, from $z = 3$ to $z = 0.9$. We find that, when parametrized in the conventional manner as $\xi_0(z) \propto (1+z)^{-(3+\epsilon)+\gamma}$, the amplitude grows with decreasing redshift, with maximum-likelihood value for the evolutionary parameter of $\epsilon = 2.05 \pm 1.0$ ($q_0 = 0.5$). When extrapolated to zero redshift, the amplitude of the correlation function implies that the correlation length $r_0 = 30^{+22}_{-13} h^{-1}$ Mpc ($q_0 = 0.5$). This suggests that strong C IV and Mg II absorbers, on megaparsec scales, are biased tracers of the higher-density regions of space, and that agglomerations of strong absorbers along a line of sight are indicators of clusters and superclusters. This is supported by recent observations of “Lyman break” galaxies. The growth seen in the clustering of absorbers is consistent with gravitationally induced growth of perturbations.

Subject headings: catalogs — cosmology: observations — intergalactic medium — large-scale structure of universe — quasars: absorption lines

¹Harlan J. Smith Postdoctoral Fellow

1. Introduction

The exact nature of QSO heavy–element absorption–line systems is not yet well understood. Nevertheless, there is growing evidence suggesting that these absorbers are associated with galaxy halos and disks. Deep images of fields around QSOs with absorbers in their spectra have been made, and galaxies have been found at the redshifts and in the vicinities of absorbers (see, e.g., Steidel, Dickenson, & Persson 1994; Steidel et al. 1997). The distances between galaxies and the associated absorbers are inferred to be of order 100 kpc, or the size of an extended galaxy halo (Churchill, Steidel, & Vogt 1996). This association has also been inferred for a substantial fraction of the Ly α absorbers (Lanzetta et al. 1995; Le Brun, Bergeron, & Boissé 1996), but they are not the subject of this work.

One approach in relating absorbers to galaxies is to compare their respective clustering properties. In a previous paper, Quashnock, Vanden Berk, & York (1996, hereafter QVY) analyzed line–of–sight correlations of C IV and Mg II absorption–line systems on large scales, using an extensive catalog of 2200 heavy–element absorption–line systems in over 500 QSO spectra (Vanden Berk et al. 1998). (More details about the catalog can be found in an earlier version of the catalog [York et al. 1991], as well as in QVY.) These authors found that the absorbers are clustered, like galaxies, on comoving scales of 50 to 100 h^{-1} Mpc ($q_0 = 0.5$).

This high–redshift (z from 1.5 to 3.5) superclustering of the absorbers is on the same comoving scale as that traced by the voids and walls of galaxy redshift surveys of the local universe (see, e.g., Kirshner et al. 1981; Geller & Huchra 1989; Landy et al. 1996). It thus appears that the absorbers are tracing the same structure as that traced by galaxies on very large scales, and that they are effective probes of very large scale structure in the universe (see, e.g., Crofts et al. 1985; Tytler, Sandoval, & Fan 1993). The authors of QVY argued that this superclustering is generic (they found potential superclusters along 7 different lines of sight); indeed, such superclustering has been detected by many studies (see, e.g., Heisler, Hogan, & White 1989; Dinshaw & Impey 1996; Williger et al. 1996; and refs. in QVY).

In this paper, we extend the QVY analysis of line–of–sight correlations of C IV and Mg II absorption–line systems to smaller comoving scales — from 1 to 16 h^{-1} Mpc, i.e., galaxy cluster scales, corresponding to line–of–sight velocity differences $\Delta v \sim 200 - 3000$ km s $^{-1}$ at $\langle z \rangle_{\text{C IV}} = 2.2$ — and relate the small–scale clustering of absorbers to galaxy clustering in general.

Early studies (Young, Sargent, & Boksenberg 1982; Sargent, Boksenberg, & Steidel 1988), with approximately 100 km s $^{-1}$ spectral resolution, found that C IV absorbers cluster significantly on these scales, with a correlation function $\xi \sim 5$ to 10 for line–of–sight velocity differences $\Delta v = 200 - 600$ km s $^{-1}$. On smaller scales ($\Delta v < 200$ km s $^{-1}$), internal motions of the gas comprising the absorption systems are expected to dominate (Heisler et al. 1989), if the absorbing gas is moving in gravitational orbits inside galactic halos with typical cloud velocity dispersions ~ 200 km s $^{-1}$ (Davis & Peebles 1983). Indeed, Petitjean & Bergeron (1994), using higher spectral resolution data, found that the C IV line–of–sight correlation function can be described by two

Gaussian components, with velocity widths $\sigma_v = 109$ and 525 km s^{-1} , with the latter component accounting for almost all (93%) of the signal in ξ for $\Delta v = 200 - 600 \text{ km s}^{-1}$. A similar result, with even higher resolution Keck High Resolution Echelle Spectrometer (HIRES) spectra, has been found by Rauch et al. (1996).

A natural interpretation (see, e.g., Sargent et al. 1988) of these results is that the low-velocity component ($\Delta v < 200 \text{ km s}^{-1}$) is due to gas motion inside the absorbers, with the higher-velocity component ($\Delta v > 200 \text{ km s}^{-1}$) being due to actual spatial clustering of the absorbers on galaxy cluster scales (several Mpc). However, because the line-of-sight velocity dispersion of typical galaxy clusters ranges from $300 - 1400 \text{ km s}^{-1}$ (Zabludoff et al. 1993; Dinshaw & Impey 1996), the higher-velocity component may represent, at least in part, motion of absorbers inside a galaxy cluster, rather than true spatial clustering (Shi 1995). This has been argued by Crofts, Burles, & Tytler (1997), who explore the spatial clustering of C IV systems along adjacent lines of sight, and claim that it is significantly weaker than clustering along a line of sight.

We return to the question of interpretation of the clustering of heavy-element absorption lines in § 6. Our interest here is in the *form* and *evolution* of that clustering on comoving scales of $1 h^{-1} \text{ Mpc}$ and greater ($\Delta v > 180 \text{ km s}^{-1}$), corresponding to the higher-velocity component. We have taken steps (§ 3) to insure that there is no aliasing of power from the low-velocity component.

The outline of the paper is as follows. We present our likelihood method of estimating the correlation function from the data in § 2. We describe our data selection criteria in § 3. We then discuss the *form* of the correlation function in § 4. We also present results on the *evolution* of the clustering, by calculating its redshift dependence in § 5. We discuss some of the implications of these results in § 6, and summarize them in § 7. In the Appendix, we explicitly calculate the likelihood as a function of data and model parameters.

2. Likelihood Method of Estimating the Absorber Correlation Function

Here we outline our likelihood method of estimating the line-of-sight correlation function, $\xi_{aa}(r, z)$. (We defer a detailed calculation of the likelihood function to the Appendix.) Unless otherwise noted, we take $q_0 = 0.5$ and $\Lambda = 0$. We follow the usual convention and take the Hubble constant to be $100 h \text{ km s}^{-1} \text{ Mpc}^{-1}$.

The correlation function $\xi_{aa}(r, z)$ relates the *observed* number of absorber pairs, separated by comoving distance r at redshift z , with the *expected* number of pairs, of the same separation and redshift, from an unclustered absorber population. The data D consist of the observed set of absorber pairs i , each with comoving separation r_i at redshift z_i . Normally, in calculating the correlation function, these data are binned, and $\xi_{aa}(r, z)$ is obtained by dividing the observed number of pairs in a bin by the number expected in the bin. In our likelihood approach, no such binning is necessary.

Consider a given model for $\xi_{\text{aa}}(r, z)$. Each such model is described by a set of parameters M , and we wish to find the parameter values which best describe the observed data D . To do so, we must maximize the *likelihood* \mathcal{L} , (calculated in the Appendix, eq. [A4]), which is the probability of the data D , given the model parameters M for the correlation function $\xi_{\text{aa}}(r, z)$: $\mathcal{L} \equiv P(D|M)$. Given a prior distribution, $P(M)$, for the model parameters (usually obtained from physical or symmetry arguments), we can use Bayes’ Theorem to then calculate the posterior probability distribution, $P(M|D)$, for the model parameters M , given the data D (see Loredo 1992 for a compendium of astrophysical applications of Bayesian inference):

$$P(M|D) = P(D|M) \times P(M) / \int P(D|M)P(M)dM . \quad (1)$$

The parameter values which maximize the likelihood are those we take as the “best-fit” values, and credible regions for the parameters around the maximum-likelihood values are obtained from equation (1), by requiring that a fiducial amount of posterior probability (such as 68.3% or 95.5%, nominal 1 and 2 σ amounts) be contained inside the credible region.

In this paper, we consider three models for the correlation function. The first is a simple power law, with comoving clustering length r_0 and power-law index γ :

$$\xi_{\text{aa}}(r, z) = (r_0/r)^\gamma . \quad (2)$$

The second is also a power law, but with an amplitude that evolves with decreasing redshift as a power of the expansion factor:

$$\xi_{\text{aa}}(r, z) = (r_0/r)^\gamma \left(\frac{1+z}{1+z_0} \right)^{-(3+\epsilon)+\gamma} . \quad (3)$$

Again r_0 is the comoving clustering length (at a fixed redshift z_0), ϵ is the conventional evolutionary parameter (Groth & Peebles 1977; Efstathiou et al. 1991), and γ is a power-law index that does not evolve with redshift. The third model is that of a power-law correlation function evolving according to linear theory of gravitational instability (Peebles 1980, 1993):

$$\xi_{\text{aa}}(r, z) = (r_0/r)^\gamma g^2(z, \Omega_0, \Lambda) , \quad (4)$$

where $g(z, \Omega_0, \Lambda)$ is the growth factor. When $\Omega_0 = 1$ and $\Lambda = 0$, $g \propto (1+z)^{-1}$.

3. Selection of the Data from the Absorber Catalog

We have drawn our C IV and Mg II data sample from the heterogeneous catalog of Vanden Berk et al. (1998) — with the aim of constructing as homogeneous a dataset as possible — by accounting for the spectral wavelength coverage, spectral sensitivity, and spectral resolution of each line of sight. The selection criteria we used to produce the final set of absorption systems are similar to those in QVY, and we outline them here.

First, the Ly α forest region, where heavy–element line identifications are often unreliable, was excluded in each spectrum. The so–called associated region, within 5000 km s $^{-1}$ of each QSO, was also excluded, because the origin of the systems in that region may be different than that of systems farther removed from the QSO (Foltz et al. 1988). Only systems with at least a C IV or Mg II doublet were selected; in that case, the intrinsically stronger doublet component was required to have been detected at the 5σ or greater significance level. In addition, a system had to have at least one more identified heavy–element line, or have a doublet equivalent width ratio that is consistent with atomic physics (within the measurement errors).

Since we are measuring correlations of absorber pairs with comoving separations of $1 h^{-1}$ Mpc or greater, we selected only those spectra or spectral regions in which the spatial resolution was better than this limit. All systems lying within $1 h^{-1}$ Mpc of each other, in the same line of sight, were combined into a single system by averaging the redshifts and taking the equivalent width of the strongest system. This has the effect of minimizing the aliasing of power from scales smaller than $1 h^{-1}$ Mpc — corresponding to $\Delta v = 180$ km s $^{-1}$ in the rest frame at $\langle z \rangle_{\text{C IV}} = 2.2$ — where internal motions of the gas comprising the absorption systems are thought to dominate (Heisler et al. 1989; and § 1 above). Since 180 km s $^{-1}$ is 1.6 times as large as the low–velocity width (Petitjean & Bergeron 1994, Fig. 4a), most of the clustering from the low–velocity Gaussian component has been removed by our selection procedure.

Applying all the selection criteria above to the Vanden Berk et al. (1998) catalog leaves a data sample consisting of 260 C IV absorbers, drawn from 202 lines of sight, with redshifts ranging from $1.2 < z < 3.6$ and mean redshift $\langle z \rangle_{\text{C IV}} = 2.2$, and 64 Mg II absorbers, drawn from 278 lines of sight, with redshifts ranging from $0.3 < z < 1.6$ and mean redshift $\langle z \rangle_{\text{Mg II}} = 0.9$.

4. Form of the Correlation Function

Figure 1 shows the line–of–sight correlation function $\xi_{\text{aa}}(r)$, for the entire sample of C IV absorbers (with mean redshift $\langle z \rangle_{\text{C IV}} = 2.2$), as a function of absorber comoving separation r from 1 to $16 h^{-1}$ Mpc, in 4 octaves. We have restricted our analysis to these scales, because data on scales larger than $16 h^{-1}$ Mpc is too scarce to be used unless it is put in very large bins, and because we did not want to examine scales smaller than $1 h^{-1}$ Mpc.

The correlation function is computed by comparing the distribution of real absorber pair separations with the expected distribution for an unclustered sample. We calculated the expected distribution using Monte Carlo simulations, creating a large number of fake unclustered catalogs, using the following “bootstrap” method (see QVY). For each Monte Carlo simulation, the same number of absorption systems as in the real sample catalog was chosen for random distribution. The redshifts and equivalent widths of the random systems were kept the same as the real systems, as were the spectral properties of the observed QSO lines of sight. The systems were then randomly placed along the lines of sight, subject to the condition that a system could have been

detected in the given line of sight. This method randomizes the absorber placements, while taking into account the redshift and equivalent width number density, which remain exactly the same as in the real sample. The expected distribution of pair separations was then calculated by averaging the pair distribution over 1000 Monte Carlo simulations. The vertical error bars through the data points are 1σ errors in the estimator for ξ_{aa} (Peebles 1980), and were computed in the same fashion as in QVY.

The first point in Figure 1 shows $\xi_{\text{aa}}(r)$ for r between 1 and $2 h^{-1}$ Mpc, corresponding to $180 - 360 \text{ km s}^{-1}$ at $\langle z \rangle_{\text{C IV}} = 2.2$. We find that $\xi_{\text{aa}} = 5.4 \pm 1.7$, a value consistent with several previous determinations: (1) $\xi_{\text{aa}} = 5.7 \pm 0.6$ for $\Delta v = 200 - 600 \text{ km s}^{-1}$ (sample A2 of Sargent et al. 1988); (2) $\xi_{\text{aa}} \sim 6$ at 360 km s^{-1} (Fig. 3 of Petitjean & Bergeron 1994); and (3) $\xi_{\text{aa}} \sim 4$ at 300 km s^{-1} (Fig. 4 of Rauch et al. 1996). However, our dataset is large enough to measure ξ_{aa} on bigger scales and to determine the form of the correlation function more accurately.

From Figure 1, the absorber line-of-sight correlation function on smaller scales can be described by a power law. However, some information has been lost because of the *binning* of data required to make the errors in Figure 1 reasonably small. Accordingly, a standard χ^2 -fit to the data is not the most powerful method available.

Instead, we have used the maximum-likelihood method of § 2 (eq. [A4]) to fit a power law of the form given in equation (2) to the *unbinned* C IV data. We find maximum-likelihood values for the parameters, obtaining $r_0 = 3.4 h^{-1}$ Mpc and $\gamma = 1.75$. This fit is shown in Figure 1, and describes the data quite well.

Figure 2 shows the credible region for these parameters. The cross marks the maximum-likelihood location, and the heavy and light contours mark the 1σ and 2σ credible regions, respectively. In calculating the credible regions, we have used Bayes' Theorem (eq. [1]) and taken uniform priors $P(M)$ in the power law intercepts to Figure 1, corresponding ² to uniform priors $P(M)$ in the parameters $\log^2 r_0$ and γ .

We condense the information in Figure 2 by showing the marginalized posterior distributions for the parameters γ and r_0 in Figures 3 and 4, respectively. The vertical lines mark the 1σ credible regions, which we find to be $1.05 < \gamma < 2.25$, and $2.4 h^{-1} \text{ Mpc} < r_0 < 4.1 h^{-1} \text{ Mpc}$ ($q_0 = 0.5$). Thus, for the C IV sample as a whole, the absorber correlation function is well-fit by a power law of the form $\xi_{\text{aa}}(r) = (r_0/r)^\gamma$, with maximum-likelihood values of $\gamma = 1.75^{+0.50}_{-0.70}$ and comoving correlation length $r_0 = 3.4^{+0.7}_{-1.0} h^{-1} \text{ Mpc}$ ($q_0 = 0.5$).

Unfortunately, the Mg II sample, with only 64 absorbers (with mean redshift $\langle z \rangle_{\text{Mg II}} = 0.9$) compared to 260 absorbers in the C IV sample, is not large enough to adequately model the form

²Since we have no *a priori* information on the scale of clustering, r_0 , nor on its overall amplitude, $\xi_{\text{aa}}(1 h^{-1} \text{ Mpc}) = r_0^\gamma$, we take uniform priors in $\log r_0$ and $\log \xi_{\text{aa}}(1 h^{-1} \text{ Mpc}) = \gamma \log r_0$ (the intercepts in Fig. 1). Thus the prior probability density $dP \propto d(\log r_0) \times d(\gamma \log r_0)$, or, using a Jacobian to change to our two independent variables of interest, γ and r_0 , $dP \propto d\gamma \times d(\log^2 r_0)$.

of the correlation function. The data are, at the 95% confidence level, consistent with all values of $\gamma > 1.55$. Nevertheless, the sample is large enough to constrain the comoving correlation length, if we fix the value of the power-law index at $\gamma = 1.75$. In this case, we find that $r_0 = 8.4 \pm 2.0 h^{-1}$ Mpc. This larger value — assuming that C IV clustering is directly comparable to that of Mg II (see § 5 below) — suggests that the amplitude of the correlation function has grown between redshift $\langle z \rangle_{\text{C IV}} = 2.2$ and redshift $\langle z \rangle_{\text{Mg II}} = 0.9$. In the following section, we find that this is indeed the case, by investigating the evolution of the correlation function, using the *entire* sample of C IV and Mg II absorbers.

5. Evolution of the Correlation Function

We have investigated the evolution of the clustering of absorbers by dividing the C IV absorber sample into three approximately equal redshift sub-samples, and comparing these to the Mg II sample. Figure 5 shows the mean of the correlation function, $\xi_0(z)$, averaged over comoving scales r from 1 to 16 h^{-1} Mpc, for the low ($1.2 < z < 2.0$), medium ($2.0 < z < 2.8$), and high ($2.8 < z < 3.6$) redshift C IV sub-samples, as well as for the Mg II sample ($0.3 < z < 1.6$). The amplitude of the correlation function is clearly growing with decreasing redshift.

We have used both the C IV and Mg II samples to study the evolution of heavy-element absorber clustering with redshift, since these samples cover almost disjoint redshift intervals. For the following reasons, we believe that it is reasonable to do this. (1) Caulet (1989), in a high-sensitivity survey of Mg II and Mg I lines found in C IV systems, found that 60% to 70% of the Mg II population ($1 < z < 2$) have moderate or strong C IV absorption lines (equivalent width $> 0.3 \text{ \AA}$, like the bulk of our sample), the rest having either weak (equivalent width $< 0.3 \text{ \AA}$) or undetected lines. Thus, Mg II systems can reasonably be expected to trace a similar clustering distribution as stronger C IV systems, and a correlation analysis should yield similar results, within the errors of $\xi_0(z)$ in Figure 5. (In the absorption catalog [Vanden Berk et al. 1998], using loose selection criteria, we find that about 67% of the Mg II systems have corresponding detected C IV lines when they were accessible. However, after applying the stricter selection criteria (§ 3) used for the clustering analysis, only 7 Mg II/C IV systems remain. This is not sufficient to directly compare the clustering of each species.) (2) The work of Petitjean & Bergeron (1990, 1994) suggests that the clustering properties of C IV and Mg II may be directly comparable. (3) It seems highly unlikely that the distribution of C IV and Mg II systems would be different, in a statistical sense, on scales as large as those studied here, i.e., 1 h^{-1} Mpc to 16 h^{-1} Mpc, corresponding to galaxy cluster and *intercluster* scales. That would imply a large-scale segregation of species. (4) The correlation function measured for Mg II systems is consistent with an extrapolation of the best-fit to the C IV data alone (see below).

We have used the maximum-likelihood formalism of § 2 and the Appendix to fit the *unbinned* C IV and Mg II data, and describe the evolution of the correlation function, using the evolving power law, given by equation (3). We fix z_0 at the mean C IV redshift of 2.2, so that the parameter

r_0 corresponds to the correlation length at that redshift, enabling a direct comparison with the results of § 3 for the C IV sample as a whole (see below). Since the data for the Mg II sample, as well as for the C IV sample as a whole, are consistent with a constant value of the power-law index γ , and since growth of hierarchical clustering in gravitational instability theory (Peebles 1980, 1993) and in numerical simulations occurs with a nearly constant value of γ , we have fixed γ at its maximum-likelihood value of 1.75 in our analysis below, and parametrized the evolution of the correlation function in terms of the evolutionary parameter ϵ and the correlation length r_0 at redshift $z_0 = 2.2$.

Figure 6 shows the credible region for these parameters. The heavy and light contours mark the 1σ and 2σ credible regions, respectively. The cross marks the maximum-likelihood location, which we find to be $\epsilon = 2.05$ and $r_0 = 3.2 h^{-1}$ Mpc. This fit is the one shown as a solid line in Figure 5.

In order to check our assumption that Mg II and C IV clustering are directly comparable, we also show the maximum-likelihood fit to the C IV data alone (shown as a dashed line in Fig. 5), which we find to be $\epsilon = 2.3$ and $r_0 = 3.3 h^{-1}$ Mpc. The correlation function measured for Mg II systems is clearly consistent with the value extrapolated from C IV at higher redshift. The error in the estimate of the evolutionary parameter ϵ is of course larger if we use the C IV data alone ($\epsilon = 2.3 \pm 1.5$); hence, we have included the Mg II data in our analysis, for the reasons given above.

We show the marginalized posterior distributions for the parameters r_0 and ϵ , in Figures 7 and 8, respectively. The vertical lines mark the 1σ credible regions, which we find to be $2.6 h^{-1} \text{ Mpc} < r_0 < 3.8 h^{-1} \text{ Mpc}$, and $1.05 < \epsilon < 3.05$. All these results are with $q_0 = 0.5$. With $q_0 = 0.1$, we expect our estimate of ϵ to decrease from 2.05 to 0.8.

It is interesting to compare the posterior distribution for r_0 in Figures 4 and 7. Both have a maximum near the same location at $r_0 \sim 3.3 h^{-1}$ Mpc, but the distribution in Figure 7 is definitely narrower. This is not surprising, since the evolution in the amplitude of the correlation function (and hence in the correlation length) has smeared the distribution of r_0 in Figure 4. There, r_0 represents the correlation length for the C IV sample as a whole (with mean redshift $\langle z \rangle_{\text{C IV}} = 2.2$), whereas in Figure 7 we have allowed for evolution, with r_0 representing the correlation length exactly at $z_0 = 2.2$. The fact that the distribution in Figure 7 is narrower is more evidence in favor of an evolving correlation function. With $\epsilon = 2.05 \pm 1.0$, the no-evolution case ($\epsilon = -1.25$) is in fact *ruled out* at the 3.3σ (99.95 %) confidence level.

6. Discussion

We have analyzed the clustering of C IV and Mg II absorption-line systems on comoving scales r from 1 to $16 h^{-1}$ Mpc, using a new likelihood method that does *not* require the usual binning used to compute the correlation function. We find that the *form* of the line-of-sight correlation function is well-described by a power law of the form $\xi_{\text{aa}}(r) = (r_0/r)^\gamma$, with maximum-likelihood

values for the power-law index of $\gamma = 1.75^{+0.50}_{-0.70}$. The clustering of absorbers at high redshift is thus of a form that is consistent with that found for galaxies and clusters, at low redshift, on megaparsec scales ($\gamma = 1.77 \pm 0.04$ for galaxies [Davis & Peebles 1983], $\gamma = 2.1 \pm 0.3$ for clusters [Nichol et al. 1992]). It appears that the absorbers are tracing the large-scale structure seen in the distribution of galaxies and clusters, and are doing so at high redshift. The finding strengthens the case for using absorbers in probing large-scale structure.

We find that the *amplitude* of the correlation function, characterized by the correlation length r_0 , is growing with decreasing redshift. For the entire C IV absorber sample, with mean redshift $\langle z \rangle_{\text{C IV}} = 2.2$, we find that $r_0 = 3.4^{+0.7}_{-1.0} h^{-1}$ Mpc ($q_0 = 0.5$), whereas for the Mg II sample, with mean redshift $\langle z \rangle_{\text{Mg II}} = 0.9$, we find that $r_0 = 8.4 \pm 2.0 h^{-1}$ Mpc. The C IV sample is large enough to be divided into several sub-samples; by using all the data sets, and parametrizing the amplitude of the correlation function in the usual manner as $\xi_0(z) \propto (1+z)^{-(3+\epsilon)+\gamma}$, we find that the growth is reflected in a value for the evolutionary parameter of $\epsilon = 2.05 \pm 1.0$ ($q_0 = 0.5$).

Evidence for a trend of increasing clustering of Ly α absorbers [with $N(\text{H I}) > 6.3 \times 10^{13} \text{ cm}^{-2}$] with decreasing redshift has been found by Cristiani et al. (1997). Like Crofts (1989), these authors also find a clear trend of increasing Ly α absorber clustering with increasing column density, and find that an extrapolation to column densities typical of heavy-element systems [$N(\text{H I}) > 10^{16} \text{ cm}^{-2}$] is consistent with the clustering observed for C IV absorbers (Petitjean & Bergeron 1994; Songaila & Cowie 1996). Our finding of growth in the clustering of heavy-element systems with decreasing redshift supports both a continuity scenario between Ly α and heavy-element systems (Crofts 1989; Tytler et al. 1995; Cowie et al. 1995; Cristiani et al. 1997), and the common action of gravitational instability.

Fernández-Soto et al. (1996) have investigated the correlation function of Ly α absorbers [with $N(\text{H I}) > 3 \times 10^{14} \text{ cm}^{-2}$] at high redshift, by using corresponding C IV systems as tracers. After comparing the observed correlations at high redshift to the galaxy correlation length at present (viz., $r_0 \sim 5.5 h^{-1}$ Mpc), they find that the evolutionary parameter ϵ is anywhere between 1.5 and 2.8 (approximate 1 σ confidence; see Fig. 4 of Fernández-Soto et al. 1996), consistent with our finding. However, their determination, unlike ours, is dependent upon comparing absorber clustering in the past with galaxy clustering at present. This is problematic, since the exact relationship between the stronger Ly α absorbers, presumed to be halos of protogalaxies, and the corresponding population of galaxies today is unknown, and different types of galaxies are known to cluster with differing strengths. Nevertheless, their determination of Ly α absorber clustering is broadly consistent with what is expected for galaxies at high redshift, and their estimate of the evolutionary parameter ϵ is consistent with ours.

The growth of the correlation function of heavy-element absorbers, as shown in Figure 5 and if extrapolated to zero redshift using the evolving power law (eq. [3]), implies a large value for the present-day value of the correlation length: $r_0 = 30^{+22}_{-13} h^{-1}$ Mpc ($q_0 = 0.5$). This value is several times larger than the average value for field galaxies today, viz., $r_0 = 5.4 \pm 1.0 h^{-1}$ Mpc (Davis &

Peebles 1983), but is comparable to that of clusters, viz., $r_0 = 16.4 \pm 4.0 h^{-1}$ Mpc (Nichol et al. 1992). The correlation length of galaxies today is known to depend on luminosity and type (Le Fèvre et al. 1996), ranging up to $7.4 h^{-1}$ Mpc in the Stromlo-APM redshift survey (Loveday et al. 1995) and up to $14.5 h^{-1}$ Mpc in the Second Southern Sky Redshift Survey (SSRS2; Benoist et al. 1996), for the most luminous early-type galaxies. Comparing all these values of the correlation length suggests that, on megaparsec scales, the strong C IV and Mg II absorbers in the Vanden Berk et al. (1998) catalog are tracing the distribution of clusters, or of the most luminous super- L_* galaxies in those clusters.

Of course, extrapolating our best fit in Figure 5 to zero redshift is highly uncertain, as reflected in the broad range in our estimate of r_0 today, and is dependent on an assumed power-law form for the evolution of the correlation function. This makes a determination of heavy-element absorber clustering at low redshift all the more important; however, the sample of low-redshift heavy-element absorption-line systems (see, e.g., Bahcall et al. 1996; Vanden Berk 1997) is too small at present to be useful in this regard.

It is not yet clear whether the correlation function shown in Figure 1 represents motion of absorbers inside a galaxy cluster (Shi 1995; Crofts, Burles, & Tytler 1997), rather than true spatial clustering, since along a line of sight we cannot distinguish peculiar velocities from the Hubble flow. In fact, on the scales considered here, the same ambiguity would arise with galaxies themselves. What is clear, however, is that the *scale* ($r_0 = 3.4 h^{-1}$ Mpc, corresponding to $\Delta v = 610 \text{ km s}^{-1}$ at $\langle z \rangle_{\text{C IV}} = 2.2$), the *form* ($\xi \propto r^{-1.75}$), and the *amplitude* of the clustering in Figure 1 all are indicative of an association of strong absorbers with clusters. Furthermore, this clustering is growing with time (Fig. 5), and could represent actual growth in spatial clustering (see below) or an increase in the velocity of absorber motions inside clusters due to increasing cluster masses.

If heavy-element absorbers are indicative of galaxy clusters, how do their number densities compare? The number of strong heavy-element absorption-line systems per unit redshift along a line of sight is $d\mathcal{N}/dz \gtrsim 1$ (see, e.g., Vanden Berk et al. 1996). Taking \bar{n} and $\bar{\sigma}$ to be, respectively, the characteristic comoving number density and effective cross section of the absorbers, and defining $d\mathcal{N}/dR$ to be the number of systems per comoving length, we obtain (Murdoch et al. 1986, $q_0 = 0.5$):

$$\bar{n}\bar{\sigma} = \frac{d\mathcal{N}}{dR} = \frac{d\mathcal{N}}{dz} \times \frac{H_0}{c} (1+z)^{\frac{3}{2}} . \quad (5)$$

Taking for an upper limit of $\bar{\sigma}$ a cross section characteristic of clusters having size an Abell radius $r_a = 1.5 h^{-1}$ Mpc, viz. $\bar{\sigma} < \pi r_a^2 = 7h^{-2} \text{ Mpc}^2$, we find that $\bar{n} > 10^{-4} h^3 \text{ Mpc}^{-3}$ at $z \gtrsim 1$ (Crofts 1989), which is at least twice the density of richness class $R \geq 0$ clusters found by Postman et al. (1996). This means there must be, *on average*, several strong heavy-element absorbers per cluster in space.

Then, if the strong clustering seen in the line-of-sight correlation function of these absorbers is indicative of clustering on galaxy cluster scales, they must be *biased* tracers of higher density regions of space. This suggests that agglomerations of strong absorbers along a line of sight

are indicators of clusters and superclusters (see QVY). This relationship is supported by the following. (1) Steidel et al. (1998) have recently discovered a large concentration of 15 “Lyman break” galaxies, at redshift $z = 3.09 \pm 0.02$, of size $11'$ by $8'$ on the plane of the sky, corresponding to $10 h^{-1}$ Mpc by $7 h^{-1}$ Mpc (comoving, $\Omega_0 = 1$). In studying the spectrum of a backlighting QSO ($z_{\text{em}} = 3.356$) that was also discovered in the field, they found a C IV doublet, as well as a strong Ly α system, at $z = 3.094$, right at the redshift of the concentration. (Two other prominent features, albeit of lower significance, were also seen in the redshift histogram of the Lyman break galaxies, and both have counterparts in metal line systems.) A similar coherence between the large-scale distribution of high-redshift galaxies ($z = 2.38$) and that of absorbing gas has also been reported by Francis et al. (1996). (2) Giavalisco et al. (1998) have estimated the amplitude of the correlation function of the aforementioned Lyman break galaxies at a median redshift $z = 3.04$, and find a correlation length $r_0 = 2.1 \pm 0.7 h^{-1}$ Mpc ($q_0 = 0.5$), a value consistent with that we have found for the C IV absorbers in Figure 5 ($r_0 = 2.2 h^{-1}$ Mpc at $z = 3.04$).

In a detailed three-dimensional numerical investigation of the evolution (from $z = 5$ to $z = 2$) of structure in the distribution of Ly α absorbers, Zhang et al. (1998) have found that the richest absorbers [$N(\text{H I}) > 10^{15} \text{ cm}^{-2}$], and, correspondingly, heavy-element systems, tend to concentrate in nodules at the intersection of filamentary structures (with comoving separation of a few megaparsecs at $z = 2$) comprising the clustering network. Those nodules appear to represent the locus of galaxy clusters. The scale of clustering found in our study of heavy-element absorption-line systems ($r_0 = 3.2 h^{-1}$ Mpc at $z = 2.2$) appears consistent with this picture, and suggests that these systems are indeed tracing the richer agglomerations of the clustering network. The previous finding by QVY of superclustering of C IV absorbers on $100 h^{-1}$ Mpc scales suggests the existence of clustering in the nodules as well.

The strong clustering that we find in the heavy-element absorption-line systems is also not surprising, given that most of the sample consists of the strongest systems with relatively large equivalent widths (order 0.4 \AA and greater), and the recent claims (Cristiani et al. 1997; D’Odorico et al. 1998) of a strong dependence of clustering strength on the column density of the systems. The median C IV $\lambda 1548$ rest equivalent width in our sample is $\langle W \rangle = 0.4 \text{ \AA}$, and there are few systems with $W < 0.1 \text{ \AA}$. We have divided the sample in half by equivalent width, and computed the mean correlation function ξ_0 averaged for comoving scales between $1 h^{-1}$ Mpc and $16 h^{-1}$ Mpc. We find that the weaker systems appear to be less clustered than the stronger systems: $\xi_0(W < 0.4 \text{ \AA}) = 0.87 \pm 0.45$, $\xi_0(W > 0.4 \text{ \AA}) = 1.73 \pm 0.60$; however, the sample size is not sufficient to significantly test the dependence of clustering on equivalent width.

The growth in the correlation function and the value of the evolutionary parameter ($\epsilon = 2.05 \pm 1.0$) that we find, are consistent with gravitationally induced growth of perturbations. For $q_0 = 0.5$, from linear theory of gravitational instability (Peebles 1980, 1993) $\xi \propto (1 + z)^{-2}$, i.e. $\epsilon = 0.75$ if $\gamma = 1.75$. Also, from numerical simulations (Melott 1992; Carlberg et al. 1997; Colin, Carlberg, & Couchman 1997), $\epsilon = 1.0 \pm 0.1$.

It is possible (eq. [4]) to examine the evolution of the correlation function, using the growth factor $g(z, \Omega_0, \Lambda)$ from linear theory of gravitational instability (Peebles 1980, 1993); however, because of the uncertainties in our determination of the evolutionary parameter ϵ and our lack of understanding of the exact nature of the heavy–element absorbers, it is not possible to derive values for the cosmological parameters Ω_0 and Λ from this work. A fruitful approach in the future may be more detailed numerical simulations of the heavy–element absorber network, like those of Zhang et al. (1998) for the Ly α forest. In addition, results from the upcoming Sloan Digital Sky Survey will add greatly to our understanding of the absorbers.

7. Summary

We summarize our results:

1. We have analyzed the clustering of C IV and Mg II absorption–line systems on comoving scales r from 1 to 16 h^{-1} Mpc, using an extensive catalog of heavy–element QSO absorbers with mean redshift $\langle z \rangle_{\text{C IV}} = 2.2$ and $\langle z \rangle_{\text{Mg II}} = 0.9$. We find that, for the C IV sample as a whole, the absorber line–of–sight correlation function is well–fit by a power law of the form $\xi_{\text{aa}}(r) = (r_0/r)^\gamma$, with maximum–likelihood values of $\gamma = 1.75^{+0.50}_{-0.70}$ and comoving $r_0 = 3.4^{+0.7}_{-1.0} h^{-1}$ Mpc ($q_0 = 0.5$).
2. The clustering of absorbers at high redshift is thus of a *form* that is consistent with that found for galaxies and clusters at low redshift, and of amplitude such that absorbers are correlated on scales of clusters of galaxies. It appears that the absorbers are tracing the large–scale structure seen in the distribution of galaxies and clusters, and are doing so at high redshift. The finding strengthens the case for using absorbers in probing large–scale structure.
3. We also trace the *evolution* of the mean amplitude $\xi_0(z)$ of the correlation function, as a function of redshift, from $z = 3$ to $z = 0.9$. We find that, when parametrized in the conventional manner as $\xi_0(z) \propto (1+z)^{-(3+\epsilon)+\gamma}$, the amplitude grows with decreasing redshift, with maximum–likelihood value for the evolutionary parameter of $\epsilon = 2.05 \pm 1.0$ ($q_0 = 0.5$).
4. When extrapolated to zero redshift, the amplitude of the correlation function implies that the correlation length $r_0 = 30^{+22}_{-13} h^{-1}$ Mpc ($q_0 = 0.5$), suggesting that strong C IV and Mg II absorbers, on megaparsec scales, are tracing the distribution of clusters of galaxies, or of the most luminous super– L_* galaxies in those clusters. The scale of clustering suggests that these absorbers are biased tracers of the higher–density regions of space, and that agglomerations of strong absorbers along a line of sight are indicators of clusters and superclusters. This is supported by recent observations of Lyman break galaxies.
5. The growth seen in the clustering of absorbers is consistent with gravitationally induced growth of perturbations.

We wish to acknowledge the long–term direction of Don York, in compiling the extensive

catalog of heavy–element absorbers used in this study and in providing intellectual leadership for the project. We acknowledge helpful discussions and useful statistical comments from Carlo Graziani. JMQ was supported in part by NASA grants GDP 93-08, NAG 5-4406, and NAG 5-2868. DEVB was supported in part by the Adler Fellowship at the University of Chicago, by NASA Space Telescope grant GO-06007.01-94A, and by the Harlan J. Smith Postdoctoral Fellowship.

A. Calculation of the Likelihood Function \mathcal{L} .

Recall that the correlation function $\xi_{\text{aa}}(r, z)$ relates the *observed* density in the number of absorber pairs, $n(r, z)$, separated by comoving distance r at redshift z , with the *expected* density in the number of pairs, $n_0(r, z)$, from an unclustered absorber population at the same separation and redshift:

$$\frac{d^2 n}{dr dz} = \frac{d^2 n_0}{dr dz} [1 + \xi_{\text{aa}}(r, z)] . \quad (\text{A1})$$

The *likelihood* \mathcal{L} is the probability of the data D , given a model (described by a set of parameters M) for the correlation function $\xi_{\text{aa}}(r, z)$: $\mathcal{L} = P(D|M)$. The data D consist of an observed set of absorber pairs i , each with comoving separation r_i at redshift z_i , contained in a small cell of size $\delta r_i \delta z_i \rightarrow 0$. We include in the likelihood not only the probability $P_i(1)$ that one pair was observed in the i th cell $\delta r_i \delta z_i$, but also the probability $P_k(0)$ that no pair was seen in the remaining empty cells $\delta r_k \delta z_k$:

$$\begin{aligned} \mathcal{L} &= \prod_i P_i(1) \times \prod_{k \neq i} P_k(0) \\ &= \prod_i \left. \frac{d^2 n}{dr dz} \right|_{(r_i, z_i)} \delta r_i \delta z_i \exp \left(- \left. \frac{d^2 n}{dr dz} \right|_{(r_i, z_i)} \delta r_i \delta z_i \right) \times \prod_{k \neq i} \exp \left(- \left. \frac{d^2 n}{dr dz} \right|_{(r_k, z_k)} \delta r_k \delta z_k \right) \\ &= \prod_i \left. \frac{d^2 n}{dr dz} \right|_{(r_i, z_i)} \delta r_i \delta z_i \times \prod_k \exp \left(- \left. \frac{d^2 n}{dr dz} \right|_{(r_k, z_k)} \delta r_k \delta z_k \right) . \end{aligned} \quad (\text{A2})$$

In taking the limit as the cell size goes to zero, and substituting equation (A1) into equation (A2), we find:

$$\begin{aligned} \log \mathcal{L} &= \lim_{\delta r_i \delta z_i \rightarrow 0} \sum_i \log \left(\left. \frac{d^2 n}{dr dz} \right|_{(r_i, z_i)} \delta r_i \delta z_i \right) - \int \int \frac{d^2 n}{dr dz} dr dz \\ &= \sum_i \log [1 + \xi_{\text{aa}}(r_i, z_i)] - \int \int \frac{d^2 n_0}{dr dz} \xi_{\text{aa}}(r, z) dr dz + C , \end{aligned} \quad (\text{A3})$$

where the constant C is just a function of the data and has no dependence on the model parameters. We compute $n_0(r, z)$ and the integral by generating a large number of simulated catalogs of unclustered absorbers, using a bootstrap Monte Carlo method described in § 4 and in

QVY. The integral term is then the mean $\langle \xi_{aa} \rangle_{\text{MC}}$ of the model correlation function, obtained by averaging $\xi_{aa}(r, z)$ over all random pairs in the Monte Carlo simulation, with r and z falling in the domain of interest:

$$\log \mathcal{L} = \sum_i \log [1 + \xi_{aa}(r_i, z_i)] - \langle \xi_{aa} \rangle_{\text{MC}} + C . \quad (\text{A4})$$

REFERENCES

- Bahcall, J. N., et al. 1996, *ApJ*, 457, 19
- Benoist, C., Maurogordato, S., da Costa, L., Cappi, A., & Schaeffer, R. 1996, *ApJ*, 472, 452
- Carlberg, R. G., Cowie, L. L., Songaila, A., & Hu, E. M. 1997, *ApJ*, 484, 538
- Caulet, A. 1989, *ApJ*, 340, 90
- Churchill, C. W., Steidel, C. C., & Vogt, S. S. 1996, *ApJ*, 471, 164
- Colin, P., Carlberg, R. G., & Couchman, H. M. P. 1997, *ApJ*, 490, 1
- Cowie, L. L., Songaila, A., & Kim, T.-S., & Hu, E. M. 1995, *AJ*, 109, 1522
- Cristiani, S., D’Odorico, S., D’Odorico, V., Fontana, A., Giallongo, E., & Savaglio, S. 1997, *MNRAS*, 285, 209
- Crotts, A. P. S., Melott, A. L., York, D. G., & Fry, J. N. 1985, *Phys. Lett. B*, 155B, 251
- Crotts, A. P. S. 1989, *ApJ*, 336, 550
- Crotts, A. P. S., Burles, S., & Tytler, D. 1997, *ApJ*, 489, L7
- Davis, M., & Peebles, P. J. E. 1983, *ApJ*, 267, 465
- Dinshaw, N., & Impey, C. D. 1996, *ApJ*, 458, 73
- D’Odorico, V., Cristiani, S., D’Odorico, S., Fontana, A., & Giallongo, E. 1998, *A&A*, in press, astro-ph/9705001
- Efstathiou, G., Bernstein, G., Katz, N., Tyson, J. A., & Guhathakurta, P. 1991, *ApJ*, 380, L47
- Fernández-Soto, A., Lanzetta, K. M., Barcons, X., Carswell, R. F., Webb, J. K., & Yahil, A. 1996, *ApJ*, 460, L85
- Foltz, C. B., Chaffee, F. H., Jr., Weymann, R. J., & Anderson, S. F. 1988, in *QSO Absorption Lines: Probing the Universe*, Proc. QSO Absorption Line Meeting, ed. J. C. Blades, D. A. Turnshek, & C. A. Norman (Cambridge: Cambridge Univ. Press), 53
- Francis, P. J., et al. 1996, *ApJ*, 457, 490
- Giavalisco, M., Steidel, C. C., Adelberger, K. L., Dickinson, M. E., Pettini, M., & Kellogg, M. 1998, *ApJ*, submitted
- Geller, M. J., & Huchra, J. P. 1989, *Science*, 246, 897
- Groth, E. J., & Peebles, P. J. E. 1977, *ApJ*, 217, 385

- Heisler, J., Hogan, C. J., & White, S. D. M. 1989, *ApJ*, 347, 52
- Kirshner, R. P., Oemler, A., Schechter, P. L., & Shectman, S. A. 1981, *ApJ*, 248, L57
- Landy, S. D., Shectman, S. A., Lin, H., Kirshner, R. P., Oemler, A. A., & Tucker, D. 1996, *ApJ*, 456, L1
- Lanzetta, K. M., Bowen, D. V., Tytler, D., Webb, J. K. 1995, *ApJ*, 442, 538
- Le Brun, V., Bergeron, J., & Boissé, P. 1996, *A&A*, 306, 691
- Le Fèvre, O., Hudon, D., Lilly, S. J., Crampton, D., Hammer, F., & Tresse, L. 1996, *ApJ*, 461, 534
- Loveday, J., Maddox, S. J., Efstathiou, G., & Peterson, B. A. 1995, *ApJ*, 442, 457
- Loredo, T. J. 1992, in *Statistical Challenges in Modern Astrophysics*, ed. E. Feigelson and G. Babu (New York: Springer-Verlag), 275
- Melott, A. L. 1992, *ApJ*, 393, L45
- Murdoch, H. S., Hunstead, R. W., Pettini, M., & Blades, J. C. 1986, *ApJ*, 309, 19
- Nichol, R. C., Collins, C. A., Guzzo, L., & Lumsden, S. L. 1992, *MNRAS*, 255, 21p
- Peebles, P. J. E. 1980, *The Large-Scale Structure of the Universe* (Princeton: Princeton Univ. Press)
- Peebles, P. J. E. 1993, *Principles of Physical Cosmology* (Princeton: Princeton Univ. Press)
- Petitjean, P., & Bergeron, J. 1990, *A&A*, 231, 309
- Petitjean, P., & Bergeron, J. 1994, *A&A*, 283, 759
- Postman, M., Lubin, L. M., Gunn, J. E., Oke, J. B., Hoessel, J. G., Schneider, D. P., Christensen, J. A. 1996, *AJ*, 111, 615
- Quashnock, J. M., Vanden Berk, D. E., & York, D. G. 1996, *ApJ*, 472, L69 (QVY)
- Rauch, M., Sargent, W. L. W., Womble, D. S., & Barlow, T. A. 1996, *ApJ*, 467, L5
- Sargent, W. L. W., Boksenberg, A., & Steidel, C. C. 1988, *ApJS*, 68, 539
- Shi, X. 1995, *ApJ*, 449, 140
- Songaila, A., Cowie, L. L. 1996, *AJ*, 112, 839
- Steidel, C. C., Dickenson, M., & Persson, S. E. 1994, *ApJ*, 437, L75
- Steidel, C. C., Dickenson, M., Meyer, D. M., Adelberger, K. L., & Sembach, K. R. 1997, *ApJ*, 480, 568

- Steidel, C. C., Adelberger, K. L., Dickenson, M., Giavalisco, M., Pettini, M., & Kellogg, M. 1998, *ApJ*, 492, 428
- Tytler, D., Sandoval, J., Fan, X.-M. 1993, *ApJ*, 405, 57
- Tytler, D., Fan, X.-M., Burles, S., Cottrell, L., Davis, C., & Kirkman, D. 1995, in *Proc. ESO Workshop, QSO Absorption Lines*, ed. G. Meylan (Heidelberg: Springer-Verlag), p. 289
- Vanden Berk, D. E., Quashnock, J. M., York, D. G., & Yanny, B. 1996, *ApJ*, 469, 78
- Vanden Berk, D. E. 1997, Ph. D. thesis (University of Chicago)
- Vanden Berk, D. E., et al. 1998, in preparation
- Williger, G. M., Hazard, C., Baldwin, J. A., & McMahon, R. G. 1996, *ApJS*, 104, 145
- York, D. G., Yanny, B., Crotts, A., Carilli, C., Garrison, E., & Matheson, L. 1991, *MNRAS*, 250, 24
- Young, P., Sargent, W. L. W., & Boksenberg, A. 1982, *ApJS*, 48, 455
- Zabludoff, A. I., Geller, M. J., Huchra, J. P., & Vogeley, M. S. 1993, *AJ*, 106, 1273
- Zhang, Y., Meiksin, A., Anninos, P., & Norman, M. L. 1998, *ApJ*, in press, astro-ph/9706087

Fig. 1.— Line-of-sight correlation function, $\xi_{\text{aa}}(r)$, for the entire sample of C IV absorbers, as a function of absorber comoving separation, r , in 4 logarithmic bins from 1 to 16 h^{-1} Mpc. The vertical error bars through the data points are 1 σ errors in the estimator for ξ_{aa} . Also shown is a power-law fit of the form $\xi_{\text{aa}}(r) = (r_0/r)^\gamma$, with maximum-likelihood values $\gamma = 1.75$ and comoving $r_0 = 3.4 h^{-1}$ Mpc ($q_0 = 0.5$).

Fig. 2.— Credible region for the parameters in the power-law fit of the form $\xi_{\text{aa}}(r) = (r_0/r)^\gamma$. The cross marks the maximum-likelihood location, at $r_0 = 3.4 h^{-1}$ Mpc ($q_0 = 0.5$) and $\gamma = 1.75$. The heavy and light contours mark the 1 σ and 2 σ credible regions, respectively.

Fig. 3.— Posterior distribution for the power-law index γ . Vertical lines mark the 1 σ credible region, $1.05 < \gamma < 2.25$.

Fig. 4.— Posterior distribution for the comoving correlation length r_0 . Vertical lines mark the 1 σ credible region, $2.4 h^{-1}$ Mpc $< r_0 < 4.1 h^{-1}$ Mpc ($q_0 = 0.5$).

Fig. 5.— Mean correlation function, $\xi_0(z)$, averaged over comoving scales r from 1 to 16 h^{-1} Mpc, as a function of redshift. Shown are values for the low ($1.2 < z < 2.0$), medium ($2.0 < z < 2.8$), and high ($2.8 < z < 3.6$) redshift C IV sub-samples, as well as for the Mg II sample ($0.3 < z < 1.6$). The solid line is a maximum-likelihood fit of the form $\xi_0(z) \propto (1+z)^{-(3+\epsilon)+\gamma}$, with $\epsilon = 2.05$ and $\gamma = 1.75$ ($q_0 = 0.5$). The dashed line is the best fit when only the C IV data are used (see text).

Fig. 6.— Credible region for the parameters in the evolving power-law fit of the form $\xi_{\text{aa}}(r, z) = (r_0/r)^\gamma \left(\frac{1+z}{1+z_0}\right)^{-(3+\epsilon)+\gamma}$. We have fixed $\gamma = 1.75$ and $z_0 = 2.2$, and $q_0 = 0.5$. The cross marks the maximum-likelihood location, at $\epsilon = 2.05$ and $r_0 = 3.2 h^{-1}$ Mpc. The heavy and light contours mark the 1 σ and 2 σ credible regions, respectively.

Fig. 7.— Posterior distribution for the comoving correlation length r_0 at redshift $z_0 = 2.2$. Vertical lines mark the 1 σ credible region, $2.6 h^{-1}$ Mpc $< r_0 < 3.8 h^{-1}$ Mpc ($q_0 = 0.5$).

Fig. 8.— Posterior distribution for the evolutionary parameter ϵ . Vertical lines mark the 1 σ credible region, $1.05 < \epsilon < 3.05$ ($q_0 = 0.5$).

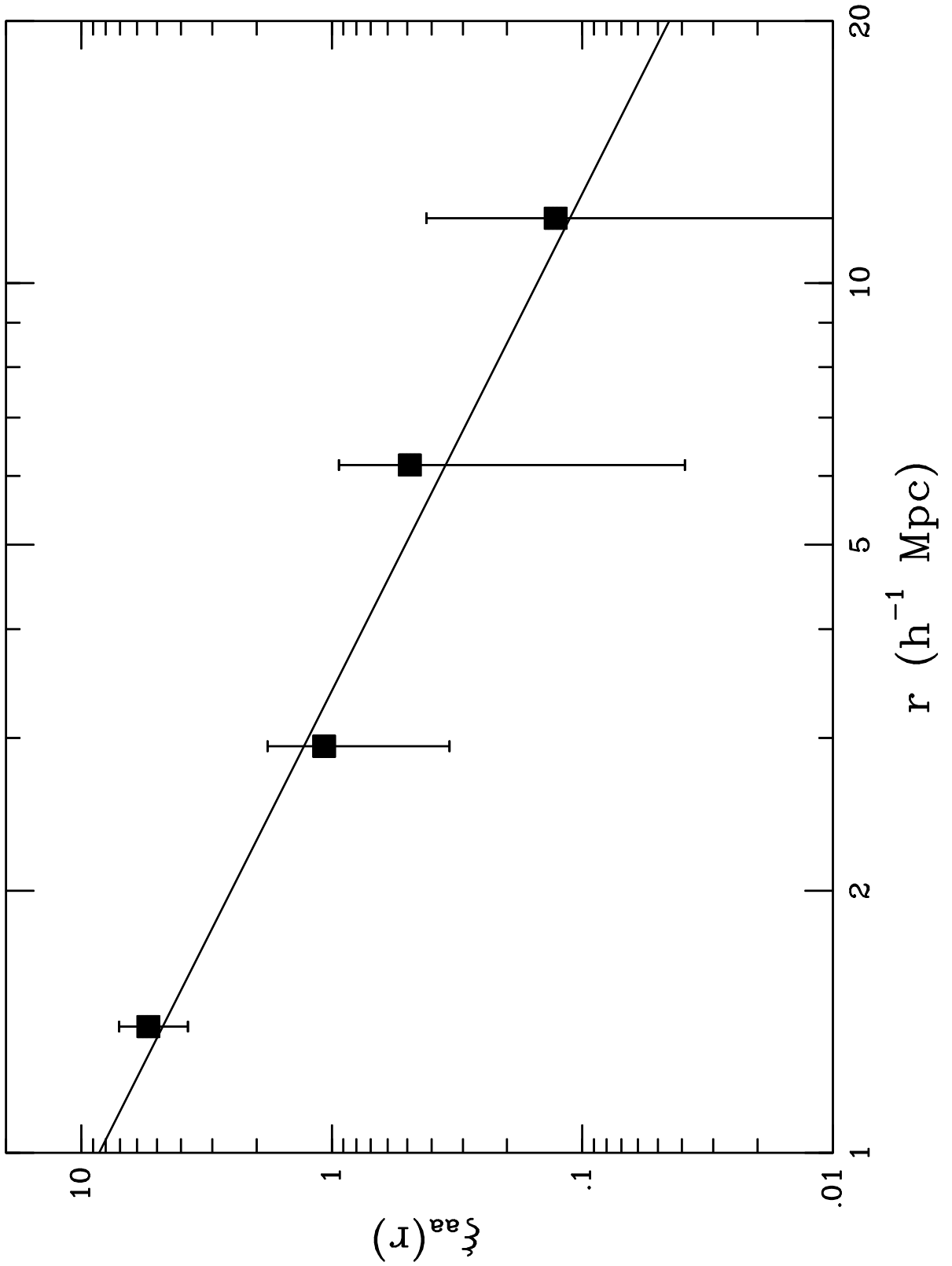


Fig. 1.—

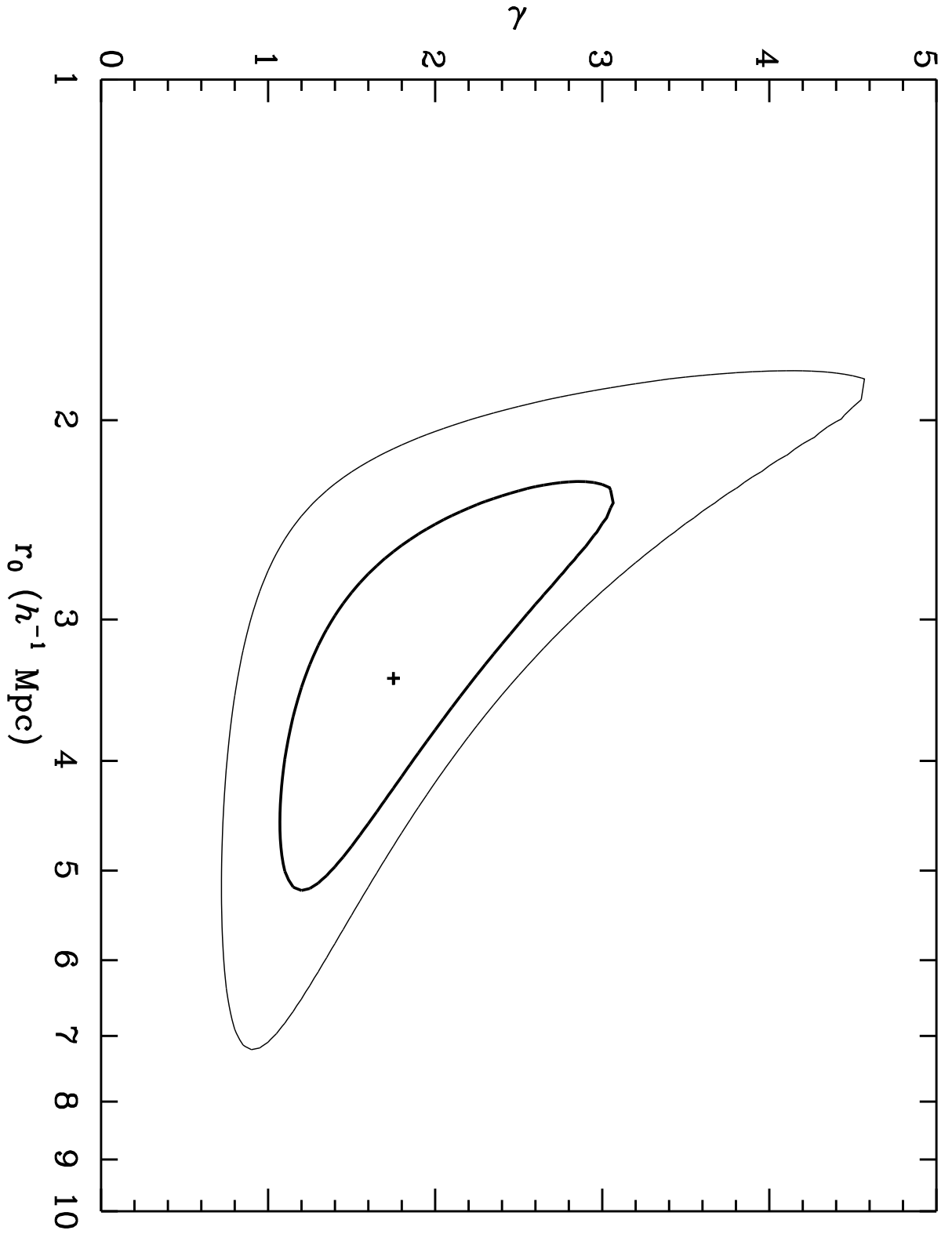


Fig. 2.—

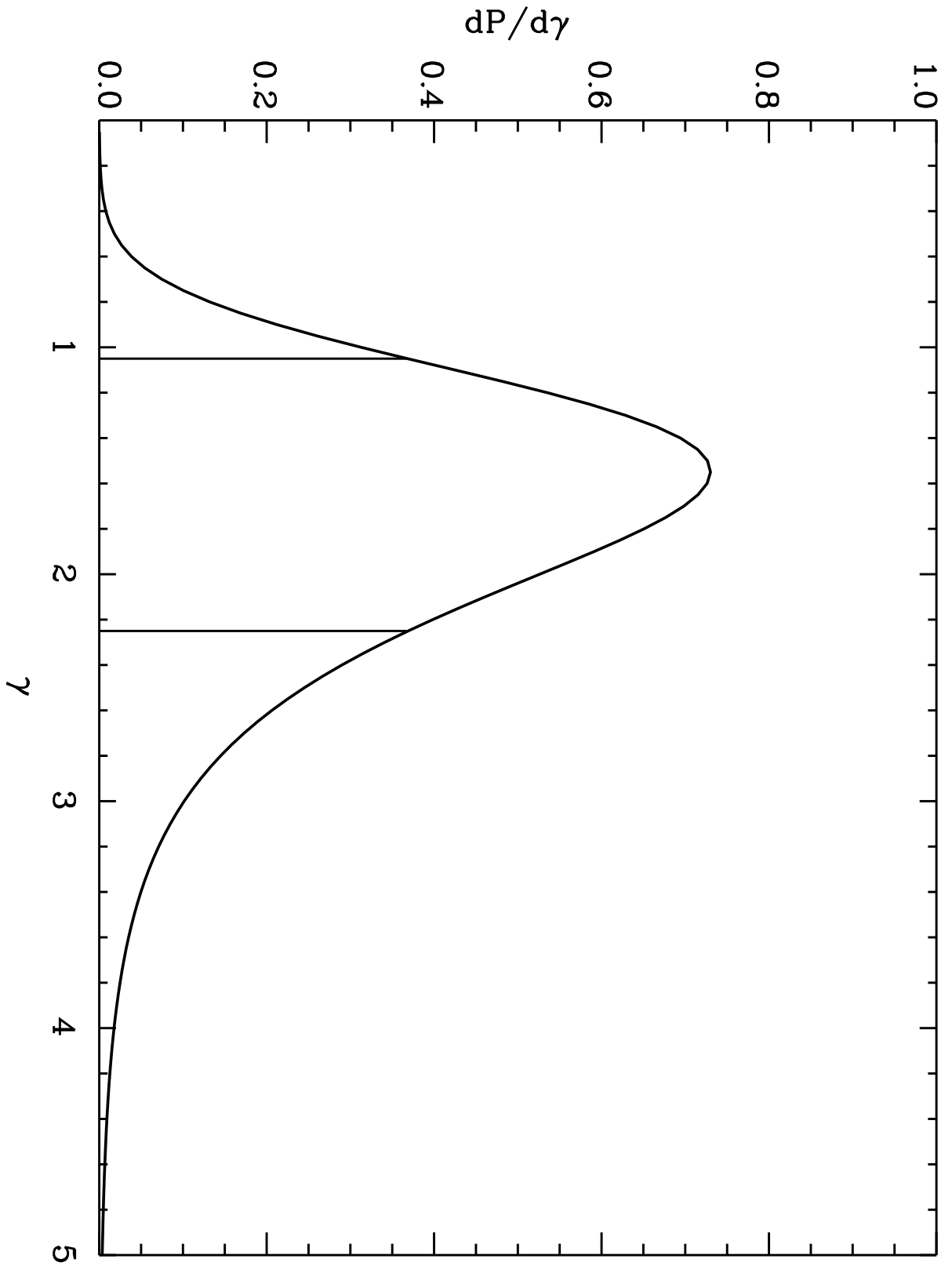


Fig. 3. —

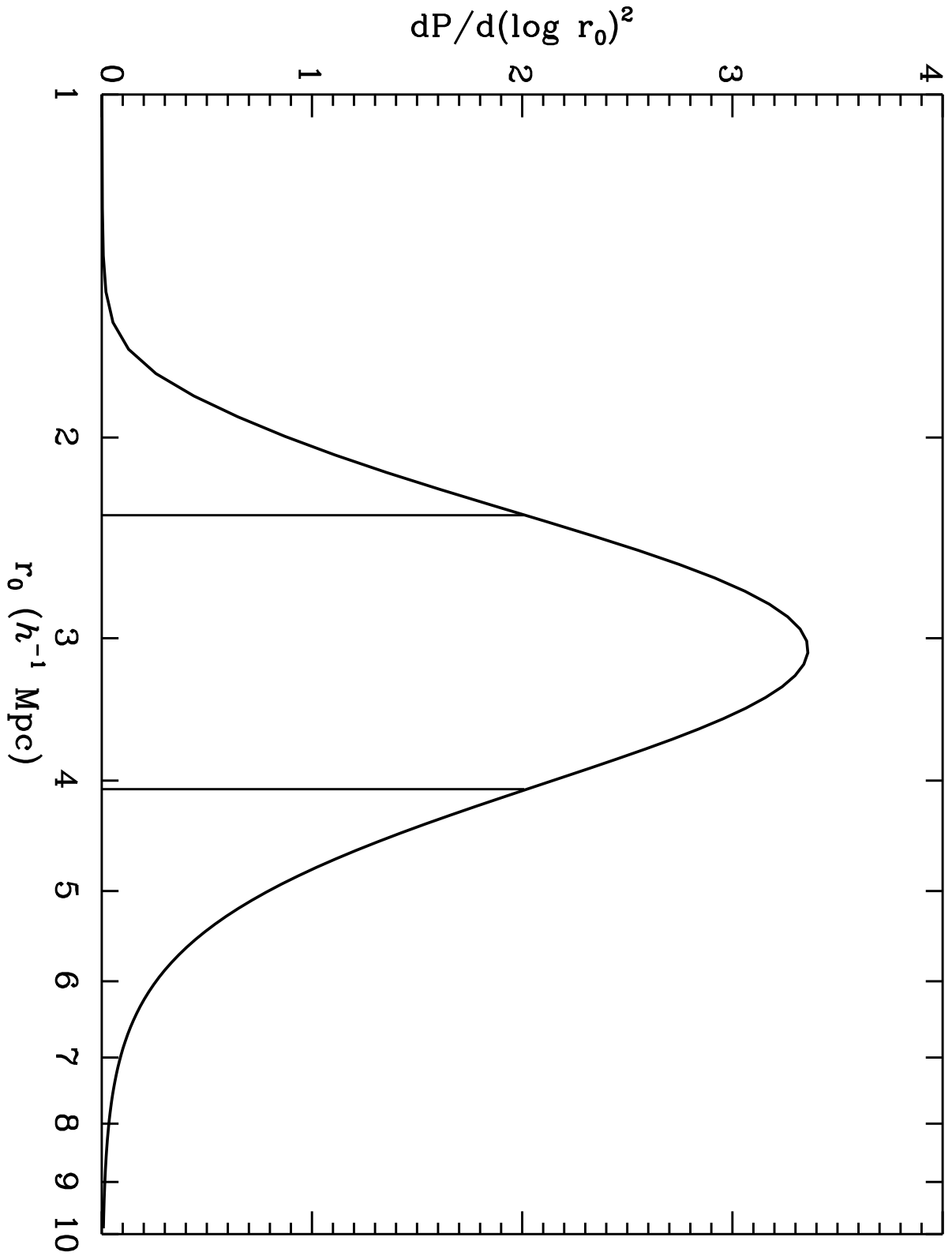


Fig. 4.—

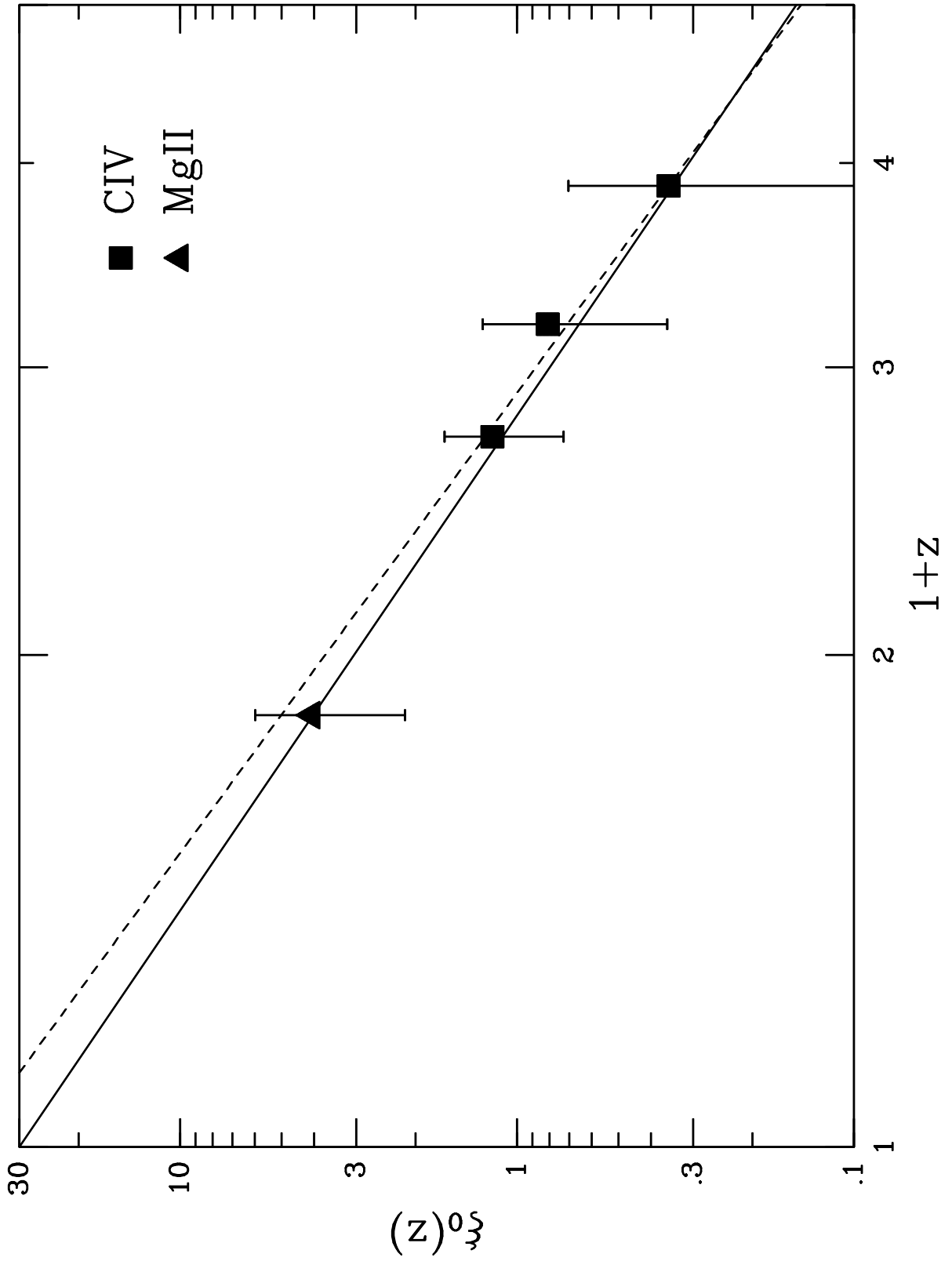


Fig. 5.—

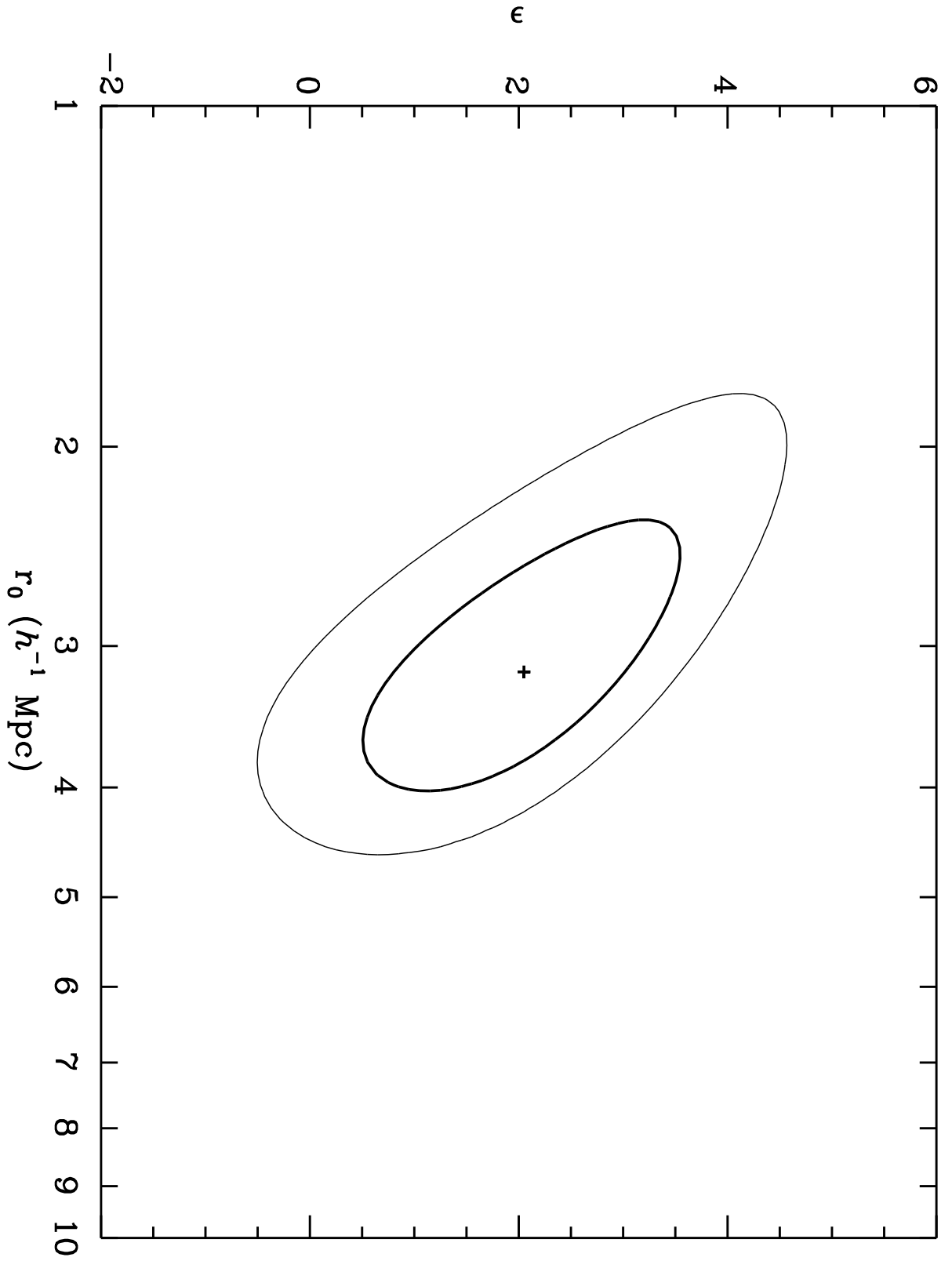


Fig. 6.—

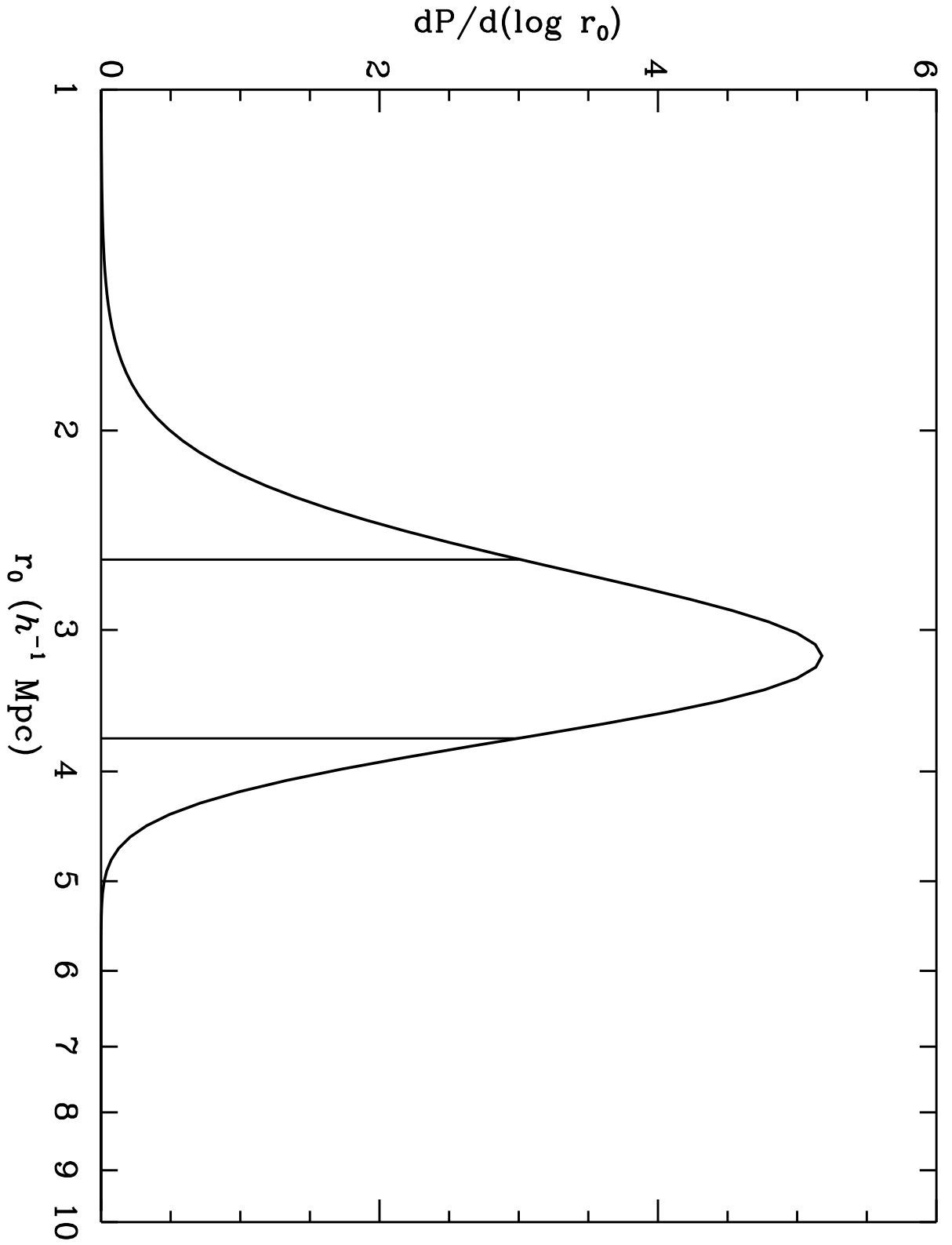


Fig. 7.—

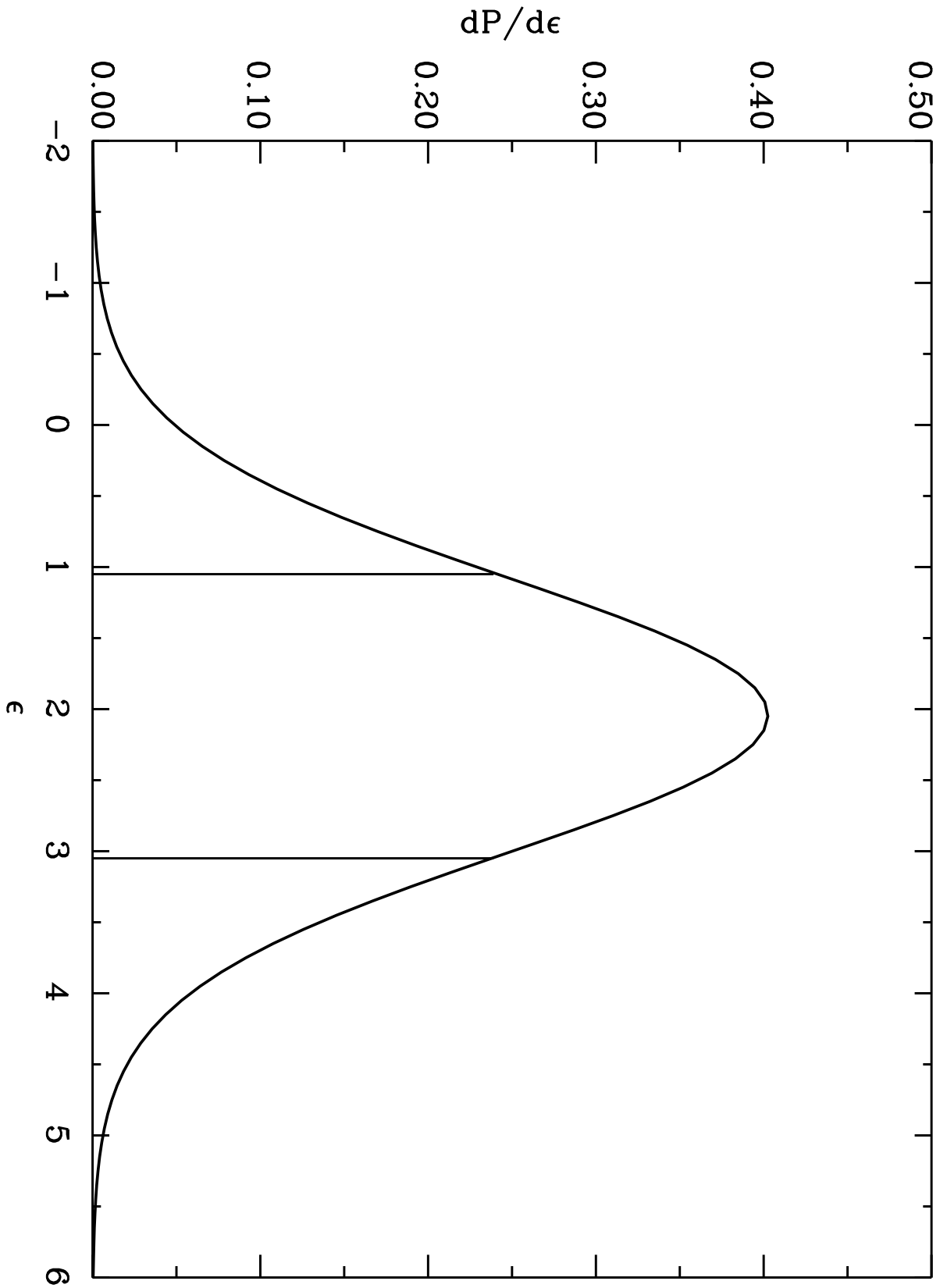


Fig. 8.—